

Eddy Currents Induced in a Finite Length Layered Rod by a Coaxial Coil

Haiyan Sun^{1,2}, John R. Bowler¹, *Senior Member, IEEE*, and Theodoros. P. Theodoulidis³, *Member, IEEE*

¹Center for Nondestructive Evaluation, Iowa State University, Ames, IA 50011-3042 USA

²GE Global Research Center, Niskayuna, NY 12309 USA

³Department of Engineering and Management of Energy Resources, University of West Macedonia, GR 50100 Kozani, Greece

We describe the calculation of eddy currents in a two-layer conducting rod of finite length excited by a coaxial circular coil carrying an alternating current. The calculation uses the truncated region eigenfunction expansion (TREE) method. By truncating the solution region to a finite length in the axial direction, we can express the magnetic vector potential as a series expansion of orthogonal eigenfunctions instead of as a Fourier integral. The restricted domain can be arbitrarily large to yield results that are as close to the infinite domain results as desired. Integral form solutions for an infinite rod are well known and relatively simple. For a finite length cylindrical conductor, however, additional boundary conditions must be satisfied at the ends. We do this by comparing series expansions term by term to match the solutions across the end of the cylinder. We derive closed-form expressions for the electromagnetic field in the presence of a finite two-layer rod. A special case of the solution is that for a conductive tube. We illustrate the end effect by calculating the coil impedance variation with respect to the axial location of the coil. The results are in very good agreement with those obtained by using a two-dimensional finite-element code.

Index Terms—Coil impedance, eddy current, eigenfunction expansion, finite rod.

I. INTRODUCTION

AN analytical solution for the electromagnetic field of a coil encircling an infinitely long cylindrical conductive rod with a uniform layer whose conductivity and permeability differed from that of the core material was given by Dodd and Deeds [1]. The solution is represented by a magnetic vector potential for each region in the form of an integral involving first-order associated Bessel functions. From the potential, other electromagnetic quantities of interest are obtained including the eddy-current density and the coil impedance. Later, Dodd *et al.* [2] generalized the solution for a coil coaxial with a cylindrical conductor having an arbitrary number of concentric homogeneous layers. The vector potential, also expressed in the form of Bessel integrals, employs a recursive relationship to link solutions in adjacent layers [2].

In this study, a theory for finite length layered rods is developed accounting for end effects using the truncated region eigenfunction expansion (TREE) method. The work is partly stimulated by the need to evaluate case depths of case hardened rods taking into account end effects. This avoids systematic errors that can arise whenever the data is interpreted using the infinite rod theory [1], [2]. There are, in fact, many other possible applications of the finite rod analysis since the results provide, for example, a simple method of calculating the impedance of a lossy inductor with a cylindrical core. The approach can also be used to calculate the demagnetization factors that have been defined for cylinders [3]. Also it can be used as an alternative to the volume element method [4], to determine the field of an axially symmetric eddy-current probe.

Truncation of the problem region to a finite length in the axial direction allows one to express the solutions in the form of series expansions that satisfy the governing equations. This can be done for a number of similar problems such as a tube with a bobbin coil inside [5], a finite homogeneous rod encircled by a coil [6], a cylindrical ferrite-cored probe in the presence of a layered conductive half space [7], or a long coil above a conductive plate with a long flaw [8].

As in the above examples, the approach here introduces an artificial boundary to limit the length of the problem domain in the axial direction. A truncation error is also introduced but it can be kept small by making the axial span as large as necessary. Another error is introduced in computation since it is necessary to limit an infinite series solution to a finite number of terms. This error is likewise easy to control and is small if a large number of terms is used, yet the computation cost remains very low compared with that needed for numerical methods. In fact, the calculation time is also small compared with that for the numerical integration to evaluate the traditional infinite rod solutions [1], [2].

The truncation of the region, and the subsequent representation of the solution as a summation of functions, classifies the TREE method as a discrete spectrum eigenfunction expansion approach. Moreover, it can be described as a meshless Galerkin method with entire domain basis functions. It is important to point out that these basis functions are solutions of the differential forms of Maxwell's equations. As a result, the method produces closed form analytical solutions for a wide range of eddy-current problems. Many numerical methods do not normally provide solutions of the governing equations. Instead, they yield numerical approximations constructed using basis functions that do not usually satisfy the electromagnetic field equations. To users of numerical code and others who are interested mainly in numerical outcomes, this may not be viewed as

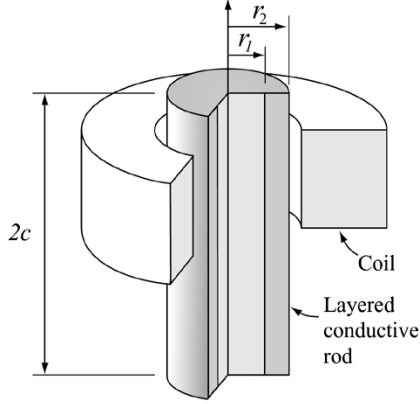


Fig. 1. Finite length cylindrical rod and a coaxial coil of rectangular cross section.

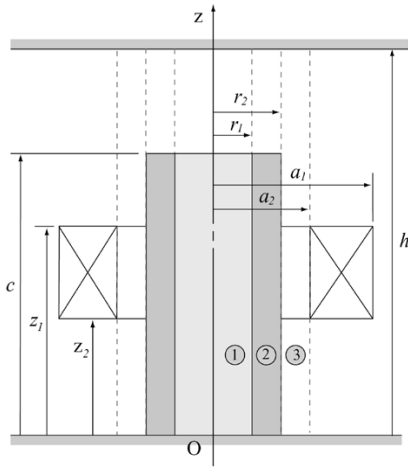


Fig. 2. Coil coaxial with a two-layer finite rod.

unsatisfactory but to many researchers, analytical solutions have a higher claim to validity and more creative possibilities but since numerical and analytical approaches are complementary, both have an important role in engineering problem solving.

II. MAGNETIC VECTOR POTENTIAL

Consider the case where the coil encircles a finite, layered conductive rod, shown in Fig. 1. We assume that the rod has two homogenous layers: an outer layer with outer radius r_2 , conductivity σ_2 , relative permeability μ_{r2} , and an inner layer with a radius r_1 , conductivity σ_1 , and relative permeability μ_{r1} . The solution domain is truncated in the axial direction to the region defined by $-h \leq z \leq h$ (Fig. 2). The electromagnetic field is represented by a magnetic vector potential with only an azimuthal component: $\mathbf{A} = \hat{\phi}A_\phi$. Assuming a time-harmonic current varying as the real part of $Ie^{-i\omega t}$, the magnetic vector potential satisfies the Laplace equation in air and the Helmholtz equation

$$(\nabla^2 + i\omega\mu_0\mu_{rn}\sigma_n) \mathbf{A} = 0 \quad n = 1, 2 \quad (1)$$

in the conductive regions 1 and 2. Solutions are of the form

$$[A \sin(qz) + B \cos(qz)] [CI_1(\gamma^{(n)}\rho) + DK_1(\gamma^{(n)}\rho)] \quad (2)$$

I_1 and K_1 are associated Bessel functions and, taking the positive root

$$\gamma^{(n)} = \sqrt{q^2 - i\omega\mu_0\mu_{rn}\sigma_n} \quad n = 1, 2. \quad (3)$$

A homogeneous Dirichlet condition

$$A_\phi(\rho, \pm h) = 0 \quad (4)$$

is applied at the boundaries, $z = \pm h$. To simplify the problem, an odd solution with respect to z , having the property $A(\rho, z) = -A(\rho, -z)$, is sought first. Then the even symmetry solution is derived following a similar procedure. Hence, only half of the solution region ($0 \leq z \leq h$) is considered at each stage. For the odd parity solution, $A_\phi(\rho, 0) = 0$ and for the even parity, $(\partial A_\phi)/(\partial z)|_{z=0} = 0$.

The odd parity solution represents the field due to a rod length $2c$ encircled by two identical coaxial coils carrying current in antiphase and located symmetrically on opposite sides of the $z = 0$ plane. If the rod is long and the coils are well separated then the electric field due to one such coil may be negligible in the $z = 0$ plane, in which case the odd parity solution gives a good approximation to the field of a single coil in the half-space that it occupies.

However, in order to represent end effects due to a short rod and a co-axial coil, one needs to average the odd and even solutions. The even parity solution represents the field due to two identical coaxial coils carrying alternating current in phase, symmetrically placed about the $z = 0$ plane. Incidentally, if the rod is long and the coils well separated, even and odd solutions should be similar in one half of the problem domain.

A. Odd Parity Solution

The magnetic vector potential, A_ϕ , in each subregion (Fig. 2), can be expanded in terms of a series of appropriate eigenfunctions

$$A_1(\rho, z) = \frac{2\mu_0 n I}{h} \sum_j \left[\begin{array}{l} \sin(q_j^{(1)} z) \\ \alpha_j^{(1)} \sin[\gamma_j^{(1)}(h-z)] \end{array} \right] \times I_1(\gamma_j^{(1)}\rho) C_j^{(1)} \quad \begin{array}{l} 0 \leq z < c \\ c \leq z \leq h \end{array} \quad (5)$$

$$A_2(\rho, z) = \frac{2\mu_0 n I}{h} \sum_j \left[\begin{array}{l} \sin(q_j^{(2)} z) \\ \alpha_j^{(2)} \sin[\gamma_j^{(2)}(h-z)] \end{array} \right] \times [I_1(\gamma_j^{(2)}\rho) C_j^{(2)} + K_1(\gamma_j^{(2)}\rho) D_j^{(2)}] \quad \begin{array}{l} 0 \leq z < c \\ c \leq z \leq h \end{array} \quad (6)$$

$$A_3(\rho, z) = \frac{2\mu_0 n I}{h} \sum_j \sin(\kappa_j z) \times [I_1(\kappa_j\rho) C_j^{(0)} + K_1(\kappa_j\rho) D_j^{(3)}] \quad 0 \leq z \leq h \quad (7)$$

where

$$\gamma_j^{(n)} = \sqrt{q_j^{(n)2} - i\omega\mu_0\mu_{rn}\sigma_n} \quad n = 1, 2 \quad (8)$$

and $n = N/[(a_1 - a_2)(z_1 - z_2)]$ is the wire turns density with N denoting the number of turns. In order to satisfy (4), $\kappa_j = j\pi/h, j = 1, 2, 3 \dots$. The eigenvalues $q_j^{(n)}$ and the coefficients $\alpha_j^{(n)}$ are defined below. One set of coefficients, the $C_j^{(0)}$, is prescribed and the solution expresses the other coefficients in terms of this set. The prescribed coefficients are found from the calculation of the vector potential, $A^{(0)}(\rho, z)$, due to a coil in the absence of the rod. The result of this preliminary calculation is [6]

$$A^{(0)}(\rho, z) = \frac{2\mu_0 n I}{h} \sum_j \sin(\kappa_j z) I_1(\kappa_j \rho) C_j^{(0)} \quad (9)$$

where

$$C_j^{(0)} = -\frac{1}{\kappa_j^3} [\cos(\kappa_j z_1) - \cos(\kappa_j z_2)] \mathcal{K}_1(\kappa_j a_1, \kappa_j a_2) \quad (10)$$

with

$$\mathcal{K}_1(x_1, x_2) = \int_{x_2}^{x_1} x K_1(x) dx. \quad (11)$$

In the steps which follow the eigenvalues, $q_j^{(n)}$, and the coefficients $\alpha_j^{(n)}$ are found by applying interface conditions at the end of the rod. Then the remaining unknown coefficients are determined by applying interface conditions at the cylindrical interfaces where $\rho = r_1$ and $\rho = r_2$. Using the continuity of H_ρ at the end of the rod, it is found that

$$\alpha_j^{(n)} = -\frac{q_j^{(n)} \cos(q_j^{(n)} c)}{\mu_{rn} \gamma_j^{(n)} \cos[\gamma_j^{(n)}(h - c)]} \quad n = 1, 2 \quad (12)$$

and from the continuity of E_ϕ at the end of the rod

$$\sin(q_j^{(n)} c) = \alpha_j^{(n)} \sin[\gamma_j^{(n)}(h - c)] \quad n = 1, 2. \quad (13)$$

Eliminating $\alpha_j^{(n)}$ gives

$$\mu_{rn} \gamma_j^{(n)} \tan(q_j^{(n)} c) + q_j^{(n)} \tan[\gamma_j^{(n)}(h - c)] = 0. \quad n = 1, 2 \quad (14)$$

from which with (8), the eigenvalues, $q_j^{(n)}$, are found by means of a numerical search for roots as described in Section V. Once the roots have been determined, the $\alpha_j^{(n)}$ can be found from (12).

Next, consider the cylindrical interfaces. From the continuity of E_ϕ and H_z at $\rho = r_1$

$$A_1 = A_2 \quad (15)$$

and

$$\left[\frac{\frac{1}{\mu_{r1}}}{1} \right] \frac{1}{\rho} \frac{\partial(\rho A_1)}{\partial \rho} \Big|_{\rho=r_1} = \left[\frac{\frac{1}{\mu_{r2}}}{1} \right] \frac{1}{\rho} \frac{\partial(\rho A_2)}{\partial \rho} \Big|_{\rho=r_1} \quad \begin{matrix} 0 \leq z < c \\ c \leq z \leq h. \end{matrix} \quad (16)$$

Similarly, from the continuity of E_ϕ and H_z at $\rho = r_2$

$$A_2 = A_3 \quad (17)$$

and

$$\left[\frac{\frac{1}{\mu_{r2}}}{1} \right] \frac{1}{\rho} \frac{\partial(\rho A_2)}{\partial \rho} \Big|_{\rho=r_2} = \left[\frac{1}{1} \right] \frac{1}{\rho} \frac{\partial(\rho A_3)}{\partial \rho} \Big|_{\rho=r_2} \quad \begin{matrix} 0 \leq z < c \\ c \leq z \leq h. \end{matrix} \quad (18)$$

Substituting (5) and (6) into (15), multiplying by $\sin(\kappa_i z)$ and integrating from zero to h gives

$$\sum_j P_{ij} I_1(\gamma_j^{(1)} r_1) C_j^{(1)} = \sum_j Q_{ij} \left[I_1(\gamma_j^{(2)} r_1) C_j^{(2)} + K_1(\gamma_j^{(2)} r_1) D_j^{(2)} \right] \quad (19)$$

where

$$P_{ij} = \int_0^c \sin(\kappa_i z) \sin(q_j^{(1)} z) dz + \alpha_j^{(1)} \int_c^h \sin(\kappa_i z) \sin[\gamma_j^{(1)}(h - z)] dz \quad (20)$$

and

$$Q_{ij} = \int_0^c \sin(\kappa_i z) \sin(q_j^{(2)} z) dz + \alpha_j^{(2)} \int_c^h \sin(\kappa_i z) \sin[\gamma_j^{(2)}(h - z)] dz. \quad (21)$$

The above integrals are evaluated using

$$\int_0^c \sin(\kappa_i z) \sin(q_j^{(n)} z) dz = \frac{\sin[(q_j^{(n)} - \kappa_i) c]}{2(q_j^{(n)} - \kappa_i)} - \frac{\sin[(q_j^{(n)} + \kappa_i) c]}{2(q_j^{(1)} + \kappa_i)} \quad n = 1, 2 \quad (22)$$

and

$$\begin{aligned} & (\gamma_j^{(n)2} - \kappa_i^2) \int_c^h \sin(\kappa_i z) \sin[\gamma_j^{(n)}(h - z)] dz \\ &= \kappa_i \cos(c\kappa_i) \sin[(c - h)\gamma_j^{(n)}] \\ & \quad - \gamma_j^{(n)} \sin(c\kappa_i) \cos[(c - h)\gamma_j^{(n)}] \quad n = 1, 2 \quad (23) \end{aligned}$$

Similarly, from (16), one gets

$$\sum_j R_{ij} \gamma_j^{(1)} I_0(\gamma_j^{(1)} r_1) C_j^{(1)} = \sum_j S_{ij} \left[\gamma_j^{(2)} I_0(\gamma_j^{(2)} r_1) C_j^{(2)} - \gamma_j^{(2)} K_0(\gamma_j^{(2)} r_1) D_j^{(2)} \right] \quad (24)$$

where

$$R_{ij} = \frac{1}{\mu_{r1}} \int_0^c \sin(\kappa_i z) \sin(q_j^{(1)} z) dz + \alpha_j^{(1)} \int_c^h \sin(\kappa_i z) \sin[\gamma_j^{(1)}(h - z)] dz \quad (25)$$

and

$$S_{ij} = \frac{1}{\mu r_2} \int_0^c \sin(\kappa_i z) \sin(q_j^{(2)} z) dz + \alpha_j^{(2)} \int_c^h \sin(\kappa_i z) \sin[\gamma_j^{(2)}(h-z)] dz. \quad (26)$$

Using the same method with (6), (7), (17), and (18), one finds that

$$\sum_j \frac{2}{h} Q_{ij} \left[I_1(\gamma_j^{(2)} r_2) C_j^{(2)} + K_1(\gamma_j^{(2)} r_2) D_j^{(2)} \right] = I_1(\kappa_j r_2) C_j^{(0)} + K_1(\kappa_j r_2) D_j^{(3)} \quad (27)$$

and

$$\sum_j \frac{2}{h} S_{ij} \left[\gamma_j^{(2)} I_0(\gamma_j^{(2)} r_2) C_j^{(2)} - \gamma_j^{(2)} K_0(\gamma_j^{(2)} r_2) D_j^{(2)} \right] = \kappa_j I_0(\kappa_j r_2) C_j^{(0)} - \kappa_j K_0(\kappa_j r_2) D_j^{(3)}. \quad (28)$$

Write (19), (24), (27), and (28) in matrix form as

$$P I_1(\gamma^{(1)} r_1) \mathbf{C}^{(1)} = \mathbf{Q} \left[I_1(\gamma^{(2)} r_1) \mathbf{C}^{(2)} + K_1(\gamma^{(2)} r_1) \mathbf{D}^{(2)} \right] \quad (29)$$

$$\mathbf{R} \gamma^{(1)} I_0(\gamma^{(1)} r_1) \mathbf{C}^{(1)} = \mathbf{S} \gamma^{(2)} \left[I_0(\gamma^{(2)} r_1) \mathbf{C}^{(2)} - K_0(\gamma^{(2)} r_1) \mathbf{D}^{(2)} \right] \quad (30)$$

$$\frac{2}{h} \mathbf{Q} \left[I_1(\gamma^{(2)} r_2) \mathbf{C}^{(2)} + K_1(\gamma^{(2)} r_2) \mathbf{D}^{(2)} \right] = I_1(\kappa r_2) \mathbf{C}^{(0)} + K_1(\kappa r_2) \mathbf{D}^{(3)} \quad (31)$$

$$\frac{2}{h} \mathbf{S} \gamma^{(2)} \left[I_0(\gamma^{(2)} r_2) \mathbf{C}^{(2)} - K_0(\gamma^{(2)} r_2) \mathbf{D}^{(2)} \right] = \kappa \left[I_0(\kappa r_2) \mathbf{C}^{(0)} - K_0(\kappa r_2) \mathbf{D}^{(3)} \right]. \quad (32)$$

Here Bessel functions with bold symbol arguments represent diagonal matrices. $\mathbf{C}^{(0)}$, $\mathbf{C}^{(1)}$, $\mathbf{C}^{(2)}$, $\mathbf{D}^{(1)}$, and $\mathbf{D}^{(2)}$ are column vectors. The four unknowns $\mathbf{C}^{(1)}$, $\mathbf{C}^{(2)}$, $\mathbf{D}^{(2)}$, and $\mathbf{D}^{(3)}$ can be expressed in terms of the known vector $\mathbf{C}^{(0)}$ using (29)–(32) by matrix and vector manipulations. The final expressions are as follows:

$$\mathbf{C}^{(1)} = \frac{h}{2} \frac{1}{r_1 r_2} \mathbf{T}^{-1} \mathbf{C}^{(0)} \quad (33)$$

$$\mathbf{C}^{(2)} = \frac{h}{2} \frac{1}{r_2} \mathbf{M}_1 \mathbf{T}^{-1} \mathbf{C}^{(0)} \quad (34)$$

$$\mathbf{D}^{(2)} = \frac{h}{2} \frac{1}{r_2} \mathbf{N}_1 \mathbf{T}^{-1} \mathbf{C}^{(0)} \quad (35)$$

$$\mathbf{D}^{(3)} = \mathbf{W} \mathbf{C}^{(0)} \quad (36)$$

where \mathbf{M}_1 , \mathbf{N}_1 , \mathbf{T} , and \mathbf{W} are defined as

$$\mathbf{M}_1 = \gamma^{(2)} K_0(\gamma^{(2)} r_1) \mathbf{Q}^{-1} P I_1(\gamma^{(1)} r_1) + K_1(\gamma^{(2)} r_1) \mathbf{S}^{-1} \mathbf{R} \gamma^{(1)} I_0(\gamma^{(1)} r_1) \quad (37)$$

$$\mathbf{N}_1 = \gamma^{(2)} I_0(\gamma^{(2)} r_1) \mathbf{Q}^{-1} P I_1(\gamma^{(1)} r_1) - I_1(\gamma^{(2)} r_1) \mathbf{S}^{-1} \mathbf{R} \gamma^{(1)} I_0(\gamma^{(1)} r_1) \quad (38)$$

$$\mathbf{M}_2 = I_1(\gamma^{(2)} r_2) \mathbf{M}_1 + K_1(\gamma^{(2)} r_2) \mathbf{N}_1 \quad (39)$$

$$\mathbf{N}_2 = I_0(\gamma^{(2)} r_2) \mathbf{M}_1 - K_0(\gamma^{(2)} r_2) \mathbf{N}_1 \quad (40)$$

$$\mathbf{T} = \kappa K_0(\kappa r_2) \mathbf{Q} \mathbf{M}_2 + K_1(\kappa r_2) \mathbf{S} \gamma^{(2)} \mathbf{N}_2 \quad (41)$$

$$\mathbf{W} = K_1^{-1}(\kappa r_2) \left[\frac{1}{r_2} \mathbf{Q} \mathbf{M}_2 \mathbf{T}^{-1} - I_1(\kappa r_2) \right]. \quad (42)$$

B. Even Parity Solution

The even parity solution can be derived following a procedure similar to that described in the previous sections. Rather than going through the derivation in full, the main distinctive features of the even parity solution are summarized below. Note that the main results of the previous section, (29)–(42), can be preserved in this form to represent either odd, even, or a linear combination of both odd and even solutions. One only needs to introduce a new set of eigenvalues for κ , q , and γ and modify the definition of the matrices \mathbf{P} , \mathbf{Q} , \mathbf{R} , and \mathbf{S} . These modifications will now be outlined.

For the even parity solution, one needs to replace the sine function in (7) for the potential in the region $0 \leq z \leq h$ by a cosine function. Similarly, for the region $0 \leq z \leq c$, the sine function in (5) and (6) is replaced by a cosine function. However, one needs to keep the sine for the solution in the region $c \leq z \leq h$, (5) and (6), because the homogeneous boundary conditions are to be satisfied at $z = h$. Thus, the magnetic vector potentials in each region for an even parity solution are given by

$$A_1(\rho, z) = \frac{2\mu_0 n I}{h} \sum_j \left[\alpha_j^{(1)} \cos(q_j^{(1)} z) \sin[\gamma_j^{(1)}(h-z)] \right] \times I_1(\gamma_j^{(1)} \rho) C_j^{(1)} \quad \begin{matrix} 0 \leq z < c \\ c \leq z \leq h \end{matrix} \quad (43)$$

$$A_2(\rho, z) = \frac{2\mu_0 n I}{h} \sum_j \left[\alpha_j^{(2)} \cos(q_j^{(2)} z) \sin[\gamma_j^{(2)}(h-z)] \right] \times \left[I_1(\gamma_j^{(2)} \rho) C_j^{(2)} + K_1(\gamma_j^{(2)} \rho) D_j^{(2)} \right] \quad \begin{matrix} 0 \leq z < c \\ c \leq z \leq h \end{matrix} \quad (44)$$

$$A_3(\rho, z) = \frac{2\mu_0 n I}{h} \sum_j \cos(\kappa_j z) \times \left[I_1(\kappa_j \rho) C_j^{(0)} + K_1(\kappa_j \rho) D_j^{(3)} \right] \quad \begin{matrix} 0 \leq z \leq h \end{matrix} \quad (45)$$

where the coefficient $C_j^{(0)}$ for an even solution is expressed as [6]

$$C_j^{(0)} = \frac{1}{\kappa_j^3} [\sin(\kappa_j z_1) - \sin(\kappa_j z_2)] \mathcal{K}_1(\kappa_j a_1, \kappa_j a_2) \quad (46)$$

and setting $\kappa_j = (2j-1)\pi/2h$, $j = 1, 2, 3, \dots$ ensures that $A_3(\rho, \pm h)$ vanishes.

From the continuity conditions that apply to the field at the end of the rod, the new eigenvalues for even symmetry are the solutions of

$$q_j^{(n)} \tan[\gamma_j^{(n)}(h-c)] - \mu_{rn} \gamma_j^{(n)} \cot[q_j^{(n)} c] = 0, \quad n = 1, 2. \quad (47)$$

Finally, it is found that the matrices \mathbf{P} , \mathbf{Q} , \mathbf{R} , and \mathbf{S} are defined in terms of the new eigenvalues for the even solution with their matrix elements, given by

$$P_{ij} = \int_0^c \cos(\kappa_i z) \cos(q_j^{(1)} z) dz + \alpha_j^{(1)} \int_c^h \cos(\kappa_i z) \sin[\gamma_j^{(1)}(h-z)] dz \quad (48)$$

$$Q_{ij} = \int_0^c \cos(\kappa_i z) \cos(q_j^{(2)} z) dz + \alpha_j^{(2)} \int_c^h \cos(\kappa_i z) \sin[\gamma_j^{(2)}(h-z)] dz \quad (49)$$

$$R_{ij} = \frac{1}{\mu_{r1}} \int_0^c \cos(\kappa_i z) \cos(q_j^{(1)} z) dz + \alpha_j^{(1)} \int_c^h \cos(\kappa_i z) \sin[\gamma_j^{(1)}(h-z)] dz \quad (50)$$

$$S_{ij} = \frac{1}{\mu_{r2}} \int_0^c \cos(\kappa_i z) \cos(q_j^{(2)} z) dz + \alpha_j^{(2)} \int_c^h \cos(\kappa_i z) \sin[\gamma_j^{(2)}(h-z)] dz \quad (51)$$

where

$$\alpha_j^{(n)} = \frac{q_j^{(n)} \sin(q_j^{(n)} c)}{\mu_{rn} \gamma_j^{(n)} \cos[\gamma_j^{(n)}(h-c)]} \quad n = 1, 2. \quad (52)$$

The integrals in (48)–(51) are evaluated as follows:

$$\int_0^c \cos(\kappa_i z) \cos(q_j^{(n)} z) dz = \frac{\sin[(q_j^{(n)} - \kappa_i) c]}{2(q_j^{(n)} - \kappa_i)} + \frac{\sin[(q_j^{(n)} + \kappa_i) c]}{2(q_j^{(1)} + \kappa_i)} \quad n = 1, 2 \quad (53)$$

$$\begin{aligned} & (\gamma_j^{(n)2} - \kappa_i^2) \int_c^h \cos(\kappa_i z) \sin[\gamma_j^{(n)}(h-z)] dz \\ &= -\gamma_j^{(n)} \cos[(c-h)\gamma_j^{(n)}] \cos(c\kappa_i) \\ & \quad - \kappa_i \sin[(c-h)\gamma_j^{(n)}] \sin(c\kappa_i) \quad n = 1, 2. \end{aligned} \quad (54)$$

This completes the evaluation of the eigenvalues and expansion coefficients for the even solution.

III. IMPEDANCE

The impedance change of a source coil due to the presence of the conductive object is given in terms of an integral over the coil region by

$$I^2 \Delta Z = - \int \Delta \mathbf{E} \cdot \mathbf{J} d\mathbf{r} \quad (55)$$

where $\Delta \mathbf{E}$ is the electric field due to eddy current in the conductor and \mathbf{J} is the coil current density. The impedance is expressed in a more convenient form for present purposes using a reciprocal relationship based on the identity

$$\begin{aligned} & \int_{\Omega} (\mathbf{b} \cdot \nabla \times \nabla \times \mathbf{a} - \mathbf{a} \cdot \nabla \times \nabla \times \mathbf{b}) d\mathbf{r} \\ &= \int_S (\mathbf{a} \times \nabla \times \mathbf{b} - \mathbf{b} \times \nabla \times \mathbf{a}) \cdot d\mathbf{S} \end{aligned} \quad (56)$$

where an arbitrary regular surface S encloses a region Ω and $d\mathbf{S} = \mathbf{n} dS$, \mathbf{n} being the outward unit normal vector. With the identifications $\mathbf{a} \equiv \mathbf{E}^{(0)}$ and $\mathbf{b} \equiv \Delta \mathbf{E}$, where the superscript (0) indicates the field in the absence of the conductor, transformation of (55) gives [9]

$$I^2 \Delta Z = \int_S (\Delta \mathbf{E} \times \mathbf{H}^{(0)} - \mathbf{E}^{(0)} \times \Delta \mathbf{H}) \cdot d\mathbf{S} \quad (57)$$

where $\Delta \mathbf{H}$ is the change in the magnetic field due to the presence of the conductor. It is emphasized that the surface S encloses the primary source, the coil in this case, and the direction of $d\mathbf{S}$ is that of an outward normal with respect to the source.

In applying the forgoing general expression, (57), to the case of the compound rod, the closed surface S will be taken to be the surface of radius r_2 co-joined with surfaces at the planes $z = \pm h$ where the field vanishes, extending outwards to join a cylindrical surface at infinity on which the surface integral vanishes. With other contributions vanishing, we need to consider only an integral over the cylinder, radius r_2 of length $2h$. With these factors taken into account, substituting the vector potential into the (57) gives

$$I^2 \Delta Z = \frac{2\pi i \omega}{\mu_0} \int_0^h \left[A^{(0)} \frac{\partial(\rho \Delta A)}{\partial \rho} - \Delta A \frac{\partial(\rho A^{(0)})}{\partial \rho} \right]_{\rho=r_2} dz. \quad (58)$$

Note that without the rod present, the magnetic vector in region 3 is given by (9) for the odd case while for the even case it is given by

$$A^{(0)}(\rho, z) = \frac{2\mu_0 n I}{h} \sum_j \cos(\kappa_j z) I_1(\kappa_j \rho) C_j^{(0)}. \quad (59)$$

With the rod present, the magnetic vector potential in this region is given by (7) for the odd case or (45) for the even case. Substituting into (58), one finds that for both odd and even cases

$$\Delta Z = -i\omega\mu_0 \frac{4\pi n^2}{h} \mathbf{C}^{(0)} \mathbf{W} \mathbf{C}^{(0)} \quad (60)$$

where \mathbf{W} is given in (42). For the odd case, $\mathbf{C}^{(0)}$ is given by (10) and for the even case by (46).

IV. TUBE

With a few modifications, the model can be applied to the problem of a tube encircled by a coaxial coil. Only the odd parity solution for a tube is given here. The even parity solution can be

derived easily using a similar procedure. Since the inner layer for a tube is air, (5) is replaced with

$$A_1(\rho, z) = 2 \frac{\mu_0 n I}{h} \sum_j \sin(\kappa_j z) I_1(\kappa_j \rho) C_j^{(1)} \quad 0 \leq z \leq h \quad (61)$$

where $\kappa_j = j\pi/h, j = 1, 2, 3 \dots$. Note that for a tube, (8), (13), and (14) are used for $n = 2$ only. From the continuity of E_ϕ and H_z at $\rho = r_1$, and with the new expression for $A_1(\rho, z)$, one finds that the definition for P_{ij} and R_{ij} should be changed to $P_{ij} = (h/2)\delta_{ij}$ and $R_{ij} = (h/2)\delta_{ij}$. Accordingly, in (29), (30), (37), and (38), one should replace \mathbf{P}, \mathbf{R} by $(h/2)\mathbf{I}$, where \mathbf{I} is a unit matrix and replace $\gamma^{(1)}$ by κ . The new expressions for these equations are listed as follows:

$$\begin{aligned} & \frac{h}{2} I_1(\kappa r_1) C^{(1)} \\ &= \mathbf{Q} \left[I_1(\gamma^{(2)} r_1) C^{(2)} + K_1(\gamma^{(2)} r_1) D^{(2)} \right] \end{aligned} \quad (62)$$

$$\begin{aligned} & \frac{h}{2} \kappa I_0(\kappa r_1) C^{(1)} \\ &= \mathbf{S} \gamma^{(2)} \left[I_0(\gamma^{(2)} r_1) C^{(2)} - K_0(\gamma^{(2)} r_1) D^{(2)} \right] \end{aligned} \quad (63)$$

$$\begin{aligned} \mathbf{M}_1 &= \frac{h}{2} \gamma^{(2)} K_0(\gamma^{(2)} r_1) \mathbf{Q}^{-1} I_1(\kappa r_1) \\ &+ \frac{h}{2} K_1(\gamma^{(2)} r_1) \mathbf{S}^{-1} \kappa I_0(\kappa r_1) \end{aligned} \quad (64)$$

$$\begin{aligned} \mathbf{N}_1 &= \frac{h}{2} \gamma^{(2)} I_0(\gamma^{(2)} r_1) \mathbf{Q}^{-1} I_1(\kappa r_1) \\ &- \frac{h}{2} I_1(\gamma^{(2)} r_1) \mathbf{S}^{-1} \kappa I_0(\gamma^{(1)} r_1). \end{aligned} \quad (65)$$

Note that for a tube, (31)–(36), (39)–(42) and (60) remain applicable.

V. EIGENVALUE CALCULATIONS

One of the critical steps is to calculate precisely the complex eigenvalues $q_j^{(n)}$ and $\gamma_j^{(n)}$, which are the roots of (14) or (47). Different approaches can be used. One method is to use the “FindRoot” function in Mathematica, using two different initial values. The first set is computed by selecting an initial value for the case $c = 0$ when $\gamma^{(n)} = \kappa$ and the second set is computed by selecting an initial value for the case $c = h$ when $\gamma^{(n)} = \sqrt{\kappa^2 + j\omega\mu\sigma}$. The two sets of computed eigenvalues are then combined to give the final set. This method works well for the odd solution of nonmagnetic material ($\mu_r = 1$).

For other cases, a similar approach to that described in [8] is used. This approach uses the Newton–Raphson method and changes c step by step. First, start with $c = 0$, in which case $\gamma = \kappa$. Then increase the rod length by a small step Δc and use the Newton–Raphson method with κ as the initial values to calculate $\gamma_i^{(n)}$ for $c = \Delta c$. Keep increasing c step by step. In each step, use $\gamma_i^{(n)}$ calculated in the previous step as the initial value, until c increases to the desired value. Another set of eigenvalues are calculated starting from $c = h$, and then decreasing c step by step. In each step, the Newton–Raphson technique is used with $\gamma_i^{(n)}$ calculated in the previous step as the initial value, until c

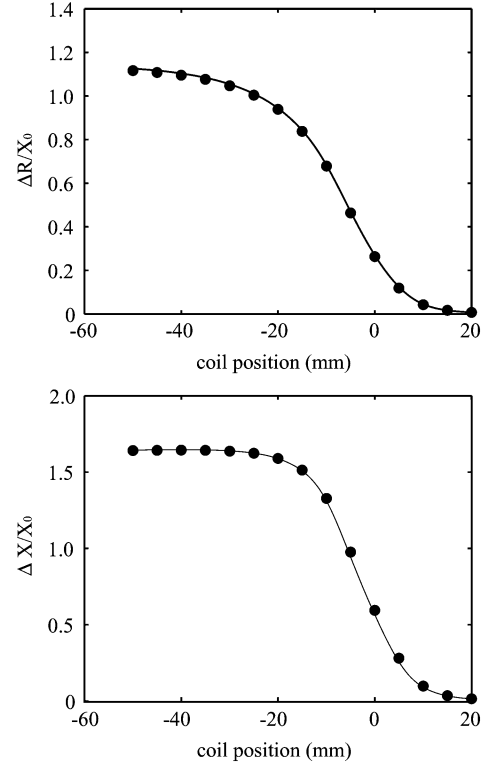


Fig. 3. Normalized coil resistance (top) and reactance (bottom) variation with position due to the two-layer steel rod at 1 kHz: comparison between TREE method (solid line) and FEMLAB result (solid circles). In the limit of an infinite rod the normalized impedance change is $1.149 + i1.632$.

decreases to the desired value. Combine the two sets of computed eigenvalues to give the complete set. With this approach, accurate eigenvalues can be obtained for magnetic material and for even solution of nonmagnetic material. More details about eigenvalue calculations are discussed in [8].

VI. RESULTS

The change of the coil impedance as it is traversed coaxially across the end of a rod and a tube is calculated using both the TREE method and a two-dimensional finite-element method (2-D FEM) package. Results are shown in Figs. 3 and 4. In these figures, the ordinate axis shows the relative distance between the coil center and the rod or tube end. Negative values mean that the center of the coil is inside the rod/tube. The results are normalized to the isolated coil reactance X_0 .

Impedance variations have been calculated for a two-layer steel rod and an aluminum tube excited at 1 kHz. The coil parameters are $a_2 = 13.7$ mm, $a_1 = 16.25$ mm, and $z_1 - z_2 = 20$ mm. The number of turns is 3200. The inner and outer radius are the same for the rod and the tube. They are $r_1 = 11.02$ mm and $r_2 = 12.69$ mm. The length of the aluminum tube is $c = 30$ mm. The length of the layered steel rod is $c = 206$ mm. The axial length of the solution region is selected to be $h = 412$ mm. The border of the region is far away from the limit of the coil movement. The material properties of the two-layer steel rod are $\sigma_1 = 5.05$ MS/m and $\mu_{r1} = 66.15$ for the inner layer and $\sigma_2 = 3.28$ MS/m and $\mu_{r2} = 37.58$ for the outer layer. The conductivity for the aluminum tube is 35.4 MS/m. The number of summation terms for evaluating the impedance is 80. For the

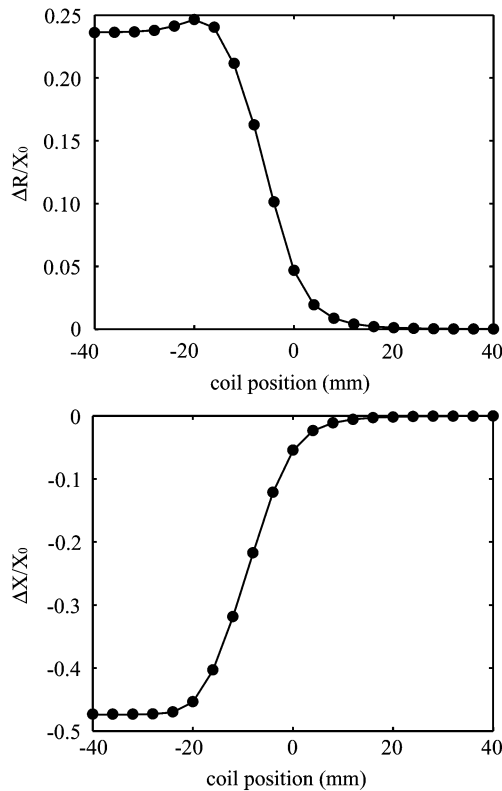


Fig. 4. Normalized coil resistance (top) and reactance (bottom) variation with position due to the short aluminum tube at 1 kHz: comparison between TREE method (solid line) and FEMLAB result (solid circles). In the limit of an infinite rod, the normalized impedance change is $0.236 - i0.474$.

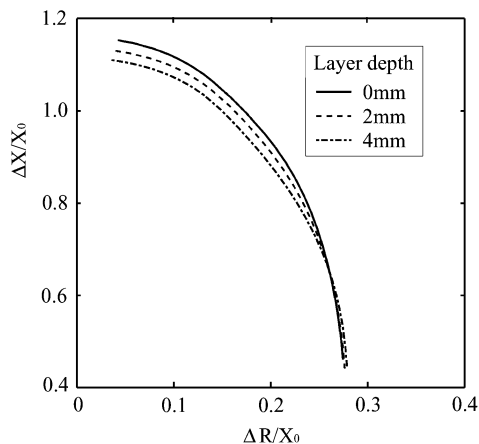


Fig. 5. Normalized coil impedance variation with frequency due to the two-layer steel rods with different outer layer depths of 0, 2, and 4 mm, respectively. The frequency varies from 6.3 to 1995.3 Hz. The coil center is placed at the end of the rod.

aluminum tube whose length is very short, both odd and even solutions are used to calculate the results but for the layered steel rod which is long compared with the coil, only the odd parity solution is used. As shown in Fig. 3, this solution is sufficient to give good results.

The normalized impedance variation with frequency has been calculated for three layered steel rods with different layer depths (Fig. 5). The frequency is varied from 6.3 to 1995.3 Hz. The

dimensions for the coil, the length, and outer radius for the rods are the same as those used for Fig. 3. The inner radius for the three rods are 8.69, 10.69, and 12.69 mm, respectively. Thus, their outer layer depths are 4, 2, and 0 mm accordingly. The coil center is located at the top end of the rod ($z = c$). Again, only the odd solution is used for the calculations.

VII. CONCLUSION

With a finite domain, the magnetic vector potential can be expressed as a series of orthogonal eigenfunctions instead of as an integral. Homogeneous boundary conditions are enforced at the boundary of the solution region. Interface conditions at the end of the rod are satisfied by comparing eigenfunctions in the series term by term. To simplify the problem, odd and even parity solutions are calculated separately. Closed-form expressions are derived using the TREE method for a two-layer rod with different material properties in each layer. The model has been modified to give the solution for a tube. The coil impedance expression is useful to allow parametric studies. The agreement with numerical results of FEM is very good. For calculating impedance variations with a fixed coil position, the speed of TREE method is comparable with the FEM method, with most of the time spent on the computation of eigenvalues and matrices which must be done at each excitation frequency. However, in case of calculating impedance variations due to different coil positions or different coil dimensions, the TREE method is much faster because the eigenvalues and the matrix W only needs to be computed once.

ACKNOWLEDGMENT

This work was supported by the NSF Industry University Collaborative Research Program at The Center for Nondestructive Evaluation, Iowa State University.

REFERENCES

- [1] C. V. Dodd and W. E. Deeds, "Analytical solutions to eddy-current probe-coil problems," *J. Appl. Phys.*, vol. 39, pp. 2829–2838, 1968.
- [2] C. V. Dodd, C. C. Cheng, and W. E. Deeds, "Induction coils coaxial with an arbitrary number of cylindrical conductors," *J. Appl. Phys.*, vol. 45, pp. 638–647, 1974.
- [3] D.-X. Chen, J. A. Brug, and R. B. Goldfarb, "Demagnetization factors for cylinders," *IEEE Trans. Magn.*, vol. 27, no. 4, pp. 3601–3617, Jul. 1991.
- [4] H. A. Sabbagh, "A model of eddy-current probes with ferrite cores," *IEEE Trans. Magn.*, vol. MAG-23, no. 3, pp. 1888–1904, May 1987.
- [5] T. P. Theodoulidis, "End effect modeling in eddy current tube testing," *Int. J. Appl. Electromagn. Mech.*, vol. 18, pp. 1–6, 2004.
- [6] J. R. Bowler and T. P. Theodoulidis, "Eddy currents induced in a conducting rod of finite length by a coaxial encircling coil," *J. Phys. D.*, vol. 38, pp. 2861–2868, 2005.
- [7] T. P. Theodoulidis, "Model of ferrite-cored probes for eddy current non-destructive evaluation," *J. Appl. Phys.*, vol. 93, no. 5, pp. 3071–3078, 2003.
- [8] T. P. Theodoulidis and J. R. Bowler, "Eddy current interaction of a long coil with a slot in a conductive plate," *IEEE Trans. Magn.*, vol. 41, no. 4, pp. 1238–1247, Apr. 2005.
- [9] B. A. Auld, "Theoretical characterization and comparison of resonant-probe microwave Eddy-current methods," in *Eddy-Current Characterization of Materials and Structures*, G. Birnbaum and G. Free, Eds: American Society for Testing and Materials, 1981, vol. STP-722, pp. 332–347.